Est. 1984

ORIENTAL JOURNAL OF CHEMISTRY
An International Open Free Access, Peer Reviewed Research Journal

www.orientjchem.org

ISSN: 0970-020 X
CODEN: OJCHEG
2017, Vol. 33, No. (1):
Pg. 296-303

Influence of pH Variation on Structural and Magnetic Properties of Ni-Zn Ferrite Nanoparticles Synthesized by Auto Combustion Method

RICHA*[1], ANAND K. TYAGI[2] and DHARAMVIR SINGH AHLAWAT[3]

[1]Department of Physics, I.K. Gujral Punjab Technical University, Jalandhar, Punjab, India.
[2]Department of Applied Sciences and Humanities,
Shaheed Bhagat Singh State Technical Campus, Ferozepur-152002, Punjab, India.
[3]Department of Physics, Chaudhary Devi Lal University, Sirsa-125055, Haryana, India.
*Correspoding author E-mail: randeepkaur02@gmail.com

http://dx.doi.org/10.13005/ojc/330135

(Received: December 20, 2016; Accepted: February 02, 2017)

ABSTRACT

Nickel zinc ferrite ($Ni_{0.5}Zn_{0.5}Fe_2O_4$) nanoparticles were synthesized via solution auto ignition combustion method. The ferrite samples were synthesized with different pH values 3, 5, 7 and 8. The as synthesized samples were calcined at 800°C for 4 hours. These synthesized nanopowder have been characterized by XRD, SEM and VSM and effect of pH value on the properties of the ferrite samples were studied. XRD pattern confirmed that samples were crystalline in nature. Crystallite size of ferrite powder increased with increase in basic nature of ferrite nanopaticles. Crystallite size of sample was found 24.86nm, 28.10nm, 33.51nm and 39.61nm at pH values 3, 5, 7 and 8 respectively. The magnetization of samples prepared at different pH values 3, 5, 7 and 8 were found 55.490e.m.u./g, 61.420e.m.u./g, 65.541e.m.u./g and 66.512e.m.u./g respectively.

Keywords: Solution-combustion method, Magnetic materials, X-ray diffraction, Magnetic properties.

INTRODUCTION

Ferrite materials draw more attention due to their unique properties[1]. Soft ferrite powder have attracted the researchers and investigators of different fields due to their numerous applications like memory system, medical science instrument etc[2-7]. Ferrites are important materials due to their various practical applications, such as magnetic storage devices[8-9]. Parameters like composition, method of synthesis, substitution of different cations, annealing time and temperature, sintered density, porosity and crystallite size alter the properties of material[10-11]. Ferrites materials are comparatively economical for preparation of various types of sensors to probe, such as magnetic field[12], current[13], gas concentrations[14-15], heat treatment[16] and mechanical stresses[17], and. Ferrite temperature sensors used in biochemical applications[18-21]. Main reasons of being ferrite samples are attracting researchers due to it's their high resistivity, applicability at higher frequency and higher corrosion resistance that

makes them highly important for high frequency applications. Different methods for synthesis of ferrite powder are co-precipitation[23], sol–gel method[22], micro emulsion method[26], hydrothermal[24, 25], reverse micelle[28], precursor[27], etc. Complex synthesis process and lower production rate are the main problems of these wet-chemical methods[29].Sol–gel auto-combustion or auto-ignition preparation method where the chemical sol–gel and ignition process is combined. This powder preparation method shown great possibility in the synthesization of spinel type ferrite nanomaterials. This method of synthesis can be considered as solution combustion technique[30]. It has been applicable for the preparation of different spinel ferrite compounds NFe_2O_4, where N could be Zn, Ni, Co, Cu, Mg, Mn ion or its combination[31–42]. Nickel-Zinc ferrites are considered as one of the most versatile soft ferrites because of its high resistance and low eddy current losses[43]. In the present course of work we have prepared the Ni-Zn ferrite (NZF) by solution auto combustion method. Normally, in ferrites nickel has a more tendency to occupy the octahedral sites whereas zinc occupies the tetrahedral site. Thus, nickel ferrite has an inverse spinel structure whereas zinc ferrite has a normal spinel structure. Hence, NZF have a mixed spinel ferrite structure. The tetrahedral sites are occupied by Zn^{2+} and Fe^{3+} whereas the octahedral sites are occupied by Ni^{2+} and Fe^{3+}. The interactions between the ions in tetrahedral and octahedral sites can alter magnetic and electrical parameters of prepared nano-ferrites. The nickel zinc ferrite properties are also dependent on the methodology adopted for their synthesis, preparative conditions like pH of solution, sintering temperature and time, chemical composition, grain size. Novelty of work is that we have prepared the nickel zinc ferrite powder by economical method. The main objective is to study the effect of pH variation on the structural and magnetic parameters of solution auto ignition synthesized NZF nanoparticles.

EXPERIEMTNAL

Materials required

Nickel Nitrate Hexahydrate, Zinc Nitrate Hexahydrate, Iron Nitrate . Nonahydrate, Citric Acid(Himeida, AR), Ammonia Solution(Sigma Aldrich, 33%).

Preparation of NZF nanoparticle

Nickel zinc ferrite ($Ni_{0.5}Zn_{0.5}Fe_2O_4$) powder samples were prepared by solution auto-combustion technique. Metal nitrates $Zn(NO_3)_2{\cdot}6H_2O$, $Ni(NO_3)_2{\cdot}6H_2O$, $Fe(NO_3)_3$. $9H_2O$ were used as starting materials. These nitrates were added separately in double distilled water and stirred for 20 minutes at 70°C[30]. Solution of citric acid in double distilled water poured into stirred metal nitrate solution, and then ammonia solution was added to continuous stirred solution for adjustment of pH value. The pH of solution was adjusted to 3, 5, 7 and 8 using ammonia solution. The mixed solution was kept onto a hot plate with continuous stirring at 100°C. After continuous approximate 7 hours of stirring the viscous brown black gel formed**.** After the formation of a highly dense sticky black brown gel, the temperature was raised to 120 °C. The temperature was then increased rapidly upto 200°C, huge amounts of gases like H_2O, CO_2 and N_2 were produced and when heated at 250-300°C, the dried gel burnt out completely to form a loose powder. The loose powder was ground in pestle motor for 30 minutes to form fine powder. Finally, the as prepared fine powder calcined at 800°C for 4 h (heating rate of 10°C/min).

Characterization Techniques

XRD

The structural parameters of synthesized NZF were investigated by X-ray diffraction (XRD; The Bruker D8 X-ray diffractometers a). The XRD pattern of samples were taken in the angle range 10-80° with 2°/min.

SEM

The morphological nautre of samples was scanned using scanning electron microscopy equipped with an energy dispersive X-ray spectrometer (SEM, JEOL).

VSM

Magnetic nature of prepared nanoparticles were studied by a vibrating sampler magnetometer (VSM PAR-155 at IIC, IIT, Roorkee) Range: 0.00001 to 10000 e.m.u., Magnetic field: 10 to +10 kOe , Temperature range : Room Temperature).

RESULTS AND DISCUSSIONS

Structural Properties

XRD

Fig.1 demonstrates the XRD pattern of NZF samples synthesized at different pH values (3, 5, 7 and 8). All the prepared samples NZ1(pH3), NZ2(pH5), NZ3(pH7) and NZ4(pH8) were crystalline in nature. The peaks of the XRD were corresponding to (111), (220), (311), (222), (400), (422), (511) and (440) planes. The highest intense peak corresponding to (311) plane. The width of diffraction maxima peaks (311) reduced and intensity of peaks increases as the pH increase. Crystallite size and crystallinity of NZF are increased with increase in pH value of samples. The crystallite size (D) was measured by using Debye Scherrer formula[44].

$$D = \frac{k\lambda}{\beta Cos\theta} \quad ...(1)$$

where k is the structure factor, b is the full width at half maxima, l is the X-Ray wavelength, q is the Brag Diffraction angle. Due to the fast combustion rate and high ignition temperature with increasing pH, higher pH produced the powder with larger crystallite size and good crystallinity. Crystallite size of sample NZ1, NZ2, NZ3 and NZ4 were

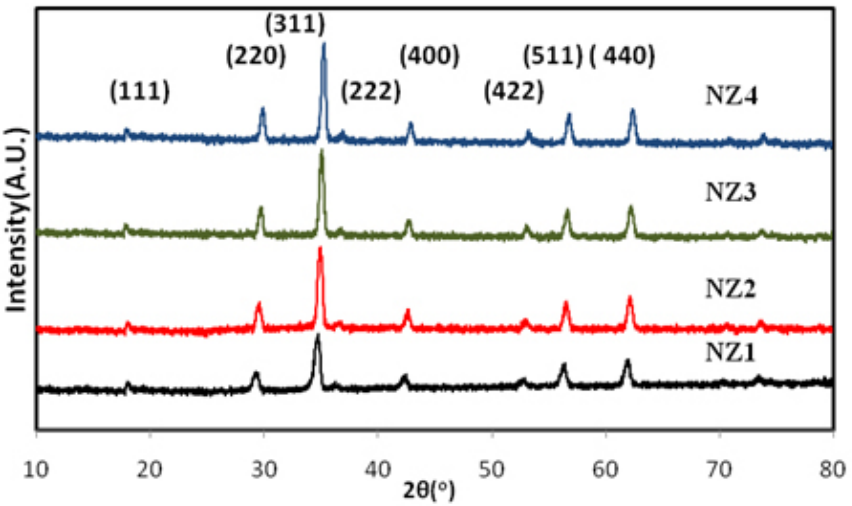

Fig. 1 XRD pattern of samples NZ1, NZ2, NZ3 and NZ4

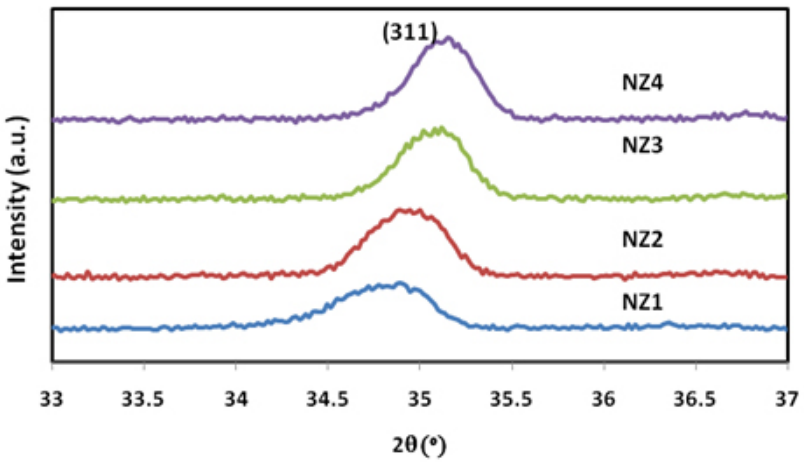

Fig. 2 XRD Peak (311) position of samples NZ1, NZ2, NZ3 and NZ4

found 24.86nm, 28.10nm, 33.51nm and 39.61nm respectively. Similar type of results was also reported by Nilar Lwin et al[45]. Fig. 2 shows the shifting of peak (311) with various pH values**.** Table 1 demonstrates the structural parameters like interplanar spacing, crystallite size of samples NZ1, NZ2, NZ3 and NZ4. Various structural parameters like crystallite size, lattice constant demonstrates in table 1.

The SEM images of heat-treated NZF are presented in Fig.3a, 3b, 3c and 3d. The SEM images demonstrates that the NZF particles have a strong tendency to hold together, forming agglomerates because of the magnetic interactions between ferrite particles during preparation process [46-47]. Grain size of NZ1, NZ2, NZ3 and NZ4 were found 24.86nm, 28.10nm, 33.51nm and 39.61nm respectively. These voids are also present in the as synthesized sample. This may be attributed to the interaction between the magnetic nanoparticles, in turn these particles grow to some extent to form larger particles at high pH of the solution[48].

Magnetic properties

The magnetic parameters of ferrites nanoparticles were altered by different parameters

Table 1: Structural parameters of samples NZ1, NZ2, NZ3 and NZ4

Sample	Peak position (°)	FWHM(°)	Crystallite size (nm)	Strain	Interplanar Spacing d (A°)	Lattice Constant (A°)
NZ1(pH3)	34.79	0.35	24.96	0.0049	2.5750	8.5440
NZ2(pH5)	34.96	0.31	28.10	0.0043	2.5641	8.5041
NZ3(pH7)	35.03	0.26	33.51	0.0036	2.5622	8.4977
NZ4(pH8)	35.10	0.22	39.61	0.0030	2.5512	8.4613

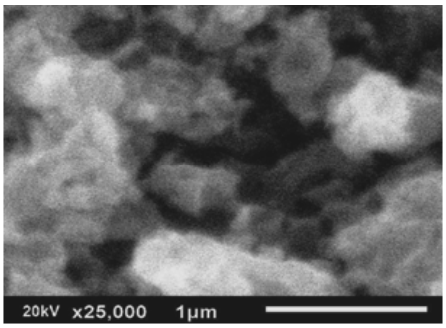

Fig. 3a: (NZ1)

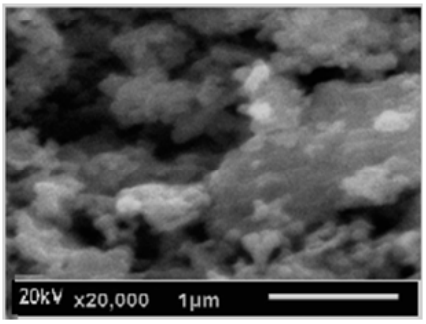

Fig.3b (NZ2)

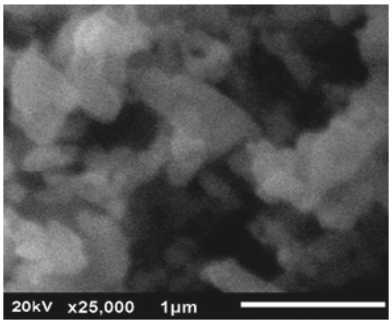

Fig.3c (NZ3)

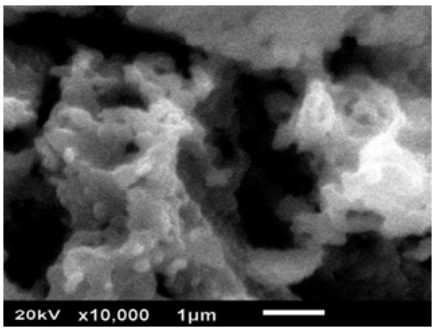

Fig.3d (NZ4)

like crystallite size, density, super exchange interactions between A and B-sites and composition. Magnetic hysteresis loops of NZF samples calcined at 800°C were obtained at room temperature by vibrating sample magnetometer (VSM) technique and are demonstrates in Fig.4 and Fig.5. The magnetic parameters like saturation magnetization, coercivity were measured from M-H loops listed in Table 2.

M-H curve of the samples show hysteresis, indicating that the samples exhibit good ferromagnetic behavior. Magnitude of magnetization of Ni-Zn ferrite nanoparticles depend on occurrence of Fe ions at A or B site. Zn^{2+} ion is non magnetic in nature merely occupies the A site. The concentration of Zn ion increases with increase of pH value from 3 to 8. Therefore when the content of Zinc is excessive,

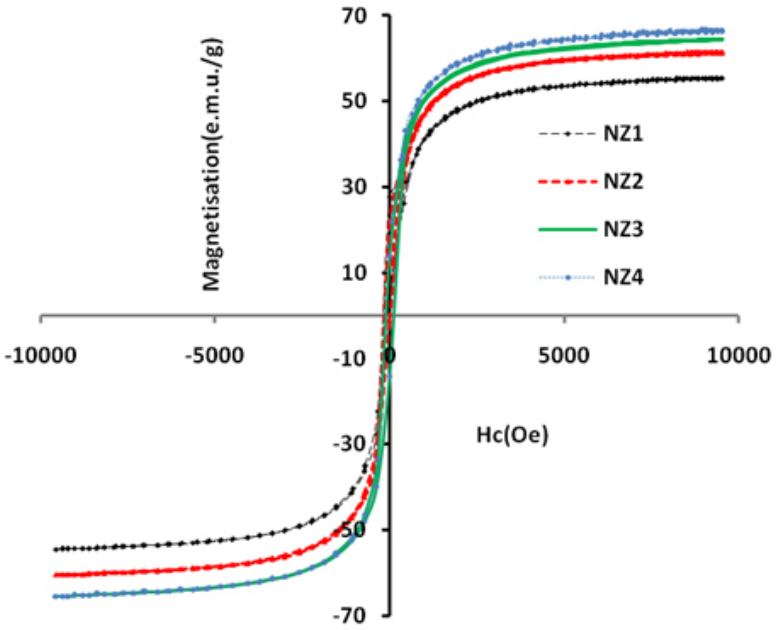

Fig. 4: M-H loops of NZ1, NZ2, NZ3 and NZ4 ferrite nanoparticles

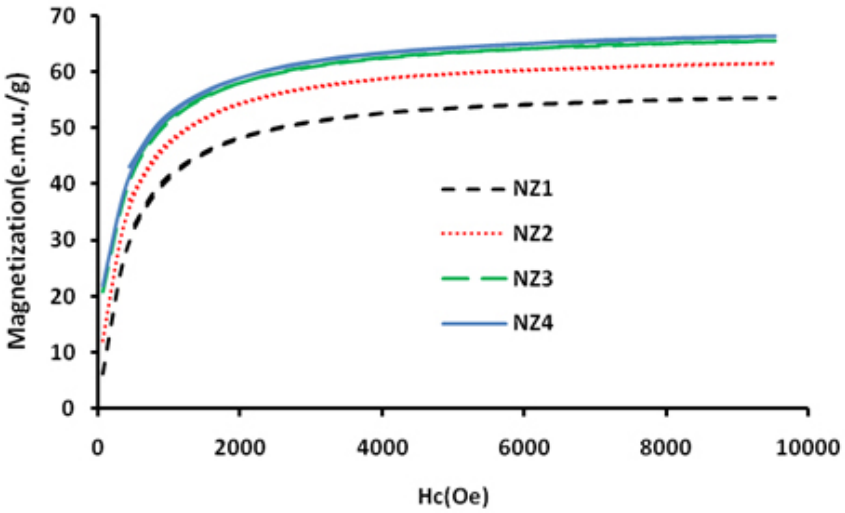

Fig. 5: M-H loops of NZ1, NZ2, NZ3 and NZ4 ferrite nanoparticles

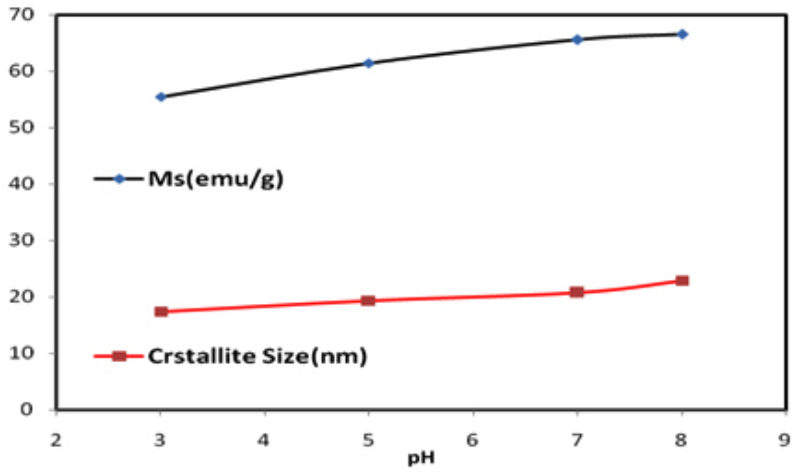

Fig. 6: Variation of crystallite size with M_s for different pH values of ferrite sample

Table 2: Magnetic parameters of samples NZ1, NZ2, NZ3 and NZ4

Sample	Saturation Magnetization (e.m.u./g)	Coercivity (Oe)
NZ1(pH3)	55.490	30.50
NZ2(pH5)	61.420	32.50
NZ3(pH7)	65.541	35.23
NZ4(pH8)	66.512	33.40

Zn^{2+} occupies most of the A site. Accordingly, the number of magnetic ion Fe is sharply reduced in the A site. More the migration of Fe^{3+} ions from A to B site results in enhancement in magnetization, due to more ions at B site as compared to A site. Hence total magnetization i.e. Ms=MB –MA increased. Nilar et. al have also reported the similar type of results[44, 49, 50]. Fig.6 demonstrates the graph between magnetization and crystallite size with different pH values 3, 5, 7 and 8.

CONCLUSIONS

The NZF samples were successfully prepared with different pH values by solution auto ignition method. The impact of pH on the magnetic and structural parameters of NZF has been investigated. The XRD results clearly shows that the crystallinity and average crystallite size of powder samples increases with an increase in pH value. Crystallite size of sample was found 24.86nm, 28.10nm, 33.51nm and 39.61nm at pH values 3, 5, 7 and 8 respectively. All the prepared samples NZ1, NZ2, NZ3 nad NZ4 are single-phase ferrites with cubic spinel structures. Auto ignition or auto combustion process resulted in the formation of nano-sized (24.86–39.61 nm), highly reactive and crystalline nickel zinc ferrite. The magnetization of samples NZ1, NZ2, NZ3 and NZ4 were measured 55.490e.m.u./g, 61.420e.m.u./g, 65.541e.m.u./g and 66.512e.m.u./g respectively.

ACKNOWLEDGEMENTS

This research work has been supported by the infrastructure of I.K. Gujral, Punjab Technical University, Jalandhar (Kapurthala). We are also very grateful to TEQIP, MHRD/World Bank Project for providing the necessary research facilities.

REFERENCES

1. Yeon, I; Kim, KD; Lee, CS.; *Physica B: Physics of Condensed Matter.* **2003**, 337, 42-51.
2. Li, S; Liu, L; John, VT; O'Connor, CJ; Harris, VG.; *IEEE Transactions on Magnetics* (New

York). **2001**, 37, 2350-2352.
3. Didukh, P.; Greneche, JM.; Slawska-Waniewska, A; Fannin, PC; Casas, LI.; *J. of Mag. and Magnetic Mat.* **2002**, 242, 613-616.
4. Neveu, S.; Bee, A.; Robineau, M.; Talbot, D.; *J. of Colloid and Interface Sci.* **2002**, 255, 293-298.
5. Rahmayeni; Zulhadjri; Jamarun, N..; Emriadi; Arief, S.; *Oriental J. Of Chem.* **2016**, 32, 1411-1419.
6. Pathmamanoharan, C.; Philipse, A.P.; *J. of Colloid and Interface Science*. **1998**, 205, 340-353.
7. Arora A. K.; Devi S.; Jaswal V. S.; Singh J.; Kinger M.; Gupta V. D. *Oriental Journal of Chemistry.* **2014**, *30,* (4), 1671-1679
8. Kumar, A.; Shrotri, P.S.; Deshpande, CE; Date, SK.; *J. of Applied Phys.* **1997**, 81, 4788–4790 .
9. Gubbala, S.; Nathani, H.; Koizol, K; Misra, R.D.K.; *J. Phys. B.* 2004, 348,317–328.
10. Parvatheeswara Rao, B.; Rao, P. S. V.; Rao, K. H.; *J. Phys.* **1997**, IV France7, CI-241.
11. Goldman, A.; Handbook of Modern Ferromagnetic Materials, *Springer Science + Business Media, New York*, **1999**.
12. Sedlar, M.; Matejec, V.; Paulicka, I.; *Sens. Act. A*, **2000,** 84, 297–302.
13. Brito, V. L. O.; Migliano, A. C. C.; Lemos, L. V.; Melo, F. C. L.; *Progress In Electromagnetics Research*, **2009**, 91, 303–318.
14. Zhang, G.; Li, C.; Cheng, F.; Chen, J.; *Sens. Act. B*, **2007,** 120, 403–410.
15. Arshak, K.; Gaidan, I.; *Mat. Sci. Eng. B* **2005**, 118, 44–49 .
16. Shin, H.-S.; *U.S. Patent No.5,* **1998,** 775, 810.
17. Bien ìkowski, A.; Szewczyc, R.; *Sens. Act. A*, **2004**, 113, 270–276.
18. Kim, Y. H.; Hashi, S.; Ishiyama, K.; Arai, K. I. ; Inoue, M.; *IEEE Trans. Magn*. **2000**, 36, 3643–3645.
19. Osada, H.; Seki, K.; Matsuki, H.; Kikuchi, S.; Murakami, K.; *IEEE Trans. Magn.* **1995***,* 31, 3164–3166.
20. Osada, H.; Chiba, S.; Oka, H.; Hatafuku, H.; Tayama, N.; Seki, K; *J. Magn. Magn. Mater*. **2004**, 272, 1761–1762.
21. Van Uitert, L. G. ; *J. Chem. Phys*. **1956,** 24, 306.
22. Gul, I. H.; Ahmed, W.; Maqsood, A.; *J. of Mag. and Magnetic Mat.* **2008**, 320, 270–275
23. Zahi, S.; Hashim, M; Daud, A. R.; *J. of Mag. and Magnetic Mat.* **2007,** 308, 177–182
24. Kosak, A.; Makovec, D.; Znidarsic, A.; *J. of the European Ceramic Soc.* **2004**, 24, 959–962
25. Jiao, X; Chen, D.; Hu, Y.; *Mate. Research Bulletin*, **2002**, 37, 1583–1588
26. Takayama, A.; Okuya, M; Kaneko, S.; *Solid State Ionics*, **2004**, 172, 257–260
27. Thakur, S; Katyal, S .C.; Singh, M.; *J. of Mag. and Magnetic Mat.* **2009**, 321, 1–7.
28. Sarangi, P .P.; Vadera, S. R.; Patra, M K; *Powder Technology* **2010**, 203, 348–353
29. Balaji, S; Kalai Selvan, K; John Berchmans, L.; *Materials Science and Engineering B*, **2005,** 119, 119–124.
30. Aruna, S T; Mukasyan, .A. S.; *Current Opinion in Solid State and Mat. Sci.* **2008**, 12, 44–50.
31. Randhawa, B S; Dosanjh, H.S.; Kumar, N.; *J. of Radio analytical and Nuclear Chem.* **2007**, 274, 581–591
32. Lee, S.P; Chen, Y.J; Ho, C.M.; *Materials Science and Engineering B* **2007**, 143, 1–6.
33. Sutka, A.; Mezinskis, G.; Pludons, A.; *Power Engi.* **2010**, 56, 254–259.
34. Sutka, A.; Gross, K. A.; Mezinskis, G.; *Physica Scripta*, **2011**, 83, 025601.
35. Thant, A. A.; Srimala, S.; Kaung, P.; *J. of the Australian Ceramic Soc.* **2010**, 46, 11–14
36. Nayak, P. K.; *Materials Chemistry and Physics* **2008,** 112, 24–26.
37. Shobana, M.K.; Rajendran, V; Jeyasubramanian, K.; *Mat. Letters* **2007**, 61, 2616–2619.
38. Mallapur, M. M; Shaikh, P.A.; Kambale, R C; *J. of Alloys and Compounds* **2009**, 479, 797–802.
39. Yue, Z.; Zhou, J.; Li, L.; *Mat. Sci. and Eng. B* **2001**, 86, 64–69.
40. Azadmanjiri, J; Salehani, H. K.; Barati, M R; *Mat. Letters* **2007**, 61, 84–87
41. Yue, Z, Zhou J, Li, L.; Zhang, H; Gui, Z; *J. of Mag. and Magnetic Mat.* **2000**, 208, 55–60.
42. Selvan, R. K.; Augustin, C. O.; Berchmans, L. J.; Saraswathi, R.; *Mat. Research Bulletin*

2003, 38, 41–54.
43. Yadoji, P.; Peelamedu, R.; Agrawal, D.; Roy, R.; *Mater. Sci.Eng. B* **2003**, 98, 269.
44. Lwin, N; Othman, R.; Noor, A.F.M.; Sreekantan, S.; Yong, T.C.; Singh, R; Tin, C.C.; , *Mat. Characterization* **2015**, 110 , 109–115
45. Bendonia, R.; Barthélémyc, A.; Sangiorgia, N.; Sangiorgia, A.; Sansona, A. *J.of Photochem. and Photobio. A: Chem.* **2016,** 330, 8–14.
46. Hsiang, H.I. ; Tsai, J.Y; *J. Mater. Sci.* **2006**, 41, 6339–6346.
47. Radyum, I.; Putri, R.A.S. ; Wahyu, B.W.; Agus, S. ; Nurul, T.R.; *Int. J. of Eng. & Tech.* **2012** 12, 5–9.
48. Gharagozlou, M.; Bayati, R; *Superlattices Microstruct.*, **2015**, *78*, 190.
49. Vijaya,K.; Paramesh, D.; Reddy, PV; *World J. Nano Sci. Eng.***2015** 7, 68–77.
50. Jia, B.; Gao, L.; *Crystal Growth Design* **2008**, 8, 1372–1376.